Supplementary Information

Ultrathin Oxygen Deficient SnO_x Films as Electron Extraction Layers for Perovskite Solar Modules

Jin-Won Lee,[1),†] Joshua Sraku Adu,[1),2),†] Raphael E. Agbenyeke,[3)] Jude Laverock,[3)] Alice Sheppard,[3)] Eunyoung Park,[1)] Youngwoong Kim,[1),4)] Soon Il Hong,[1)] Nam Joong Jeon,[1),] David J. Fermin,[3),*] and Helen Hejin Park[1),2),*]*

[1)] Advanced Materials Division, Korea Research Institute of Chemical Technology (KRICT), Daejeon, Republic of Korea 34114

[2)] Department of Advanced Materials and Chemical Engineering, University of Science and Technology (UST), Daejeon, Republic of Korea 34113

[3)] School of Chemistry, University of Bristol, Bristol BS8 1TL, United Kingdom

[4)] Green and Sustainable Materials R&D Department, Korea Institute of Industrial Technol ogy (KITECH), Cheonan, Chungcheongnam-do 31056, Republic of Korea

AUTHOR INFORMATION

[†] These authors contributed equally to this work.

Corresponding Authors

[*] E-mail: hhpark@krict.re.kr, david.fermin@bristol.ac.uk, njjeon@krict.re.kr

S1. EXPERIMENTAL SECTION

1.1 Materials

Materials used in the experiments include, tin oxide (Alfa), home-made formamidinium lead iodide ($FAPbI_3$) black powder (KRICT), home-made methylammonium bromide ($MAPbBr_3$), methylammonium chloride (MACl, Sigma-Aldrich), poly(triarylamine) (PTAA) (MS Solution), *N*,*N*-dimethylformamide (DMF; 99.8%, Sigma-Aldrich), dimethyl sulfoxide (DMSO; 99.9%, Sigma-Aldrich), chlorobenzene (99.8%, Sigma-Aldrich), toluene (99.8%, Sigma-Aldrich), 2-methoxyethanol (2-ME; 99.8%, Sigma-Aldrich), ethanol (99.9%, DUKSAN PURE CHEMICALS), and ethylacetate (99.0%, DUKSAN PURE CHEMICALS).

1.2 Fabrication of perovskite unit cells

As transparent electrodes, glass/ITO (indium tin oxide on glass) substrates were prepared by cleaning with a special detergent followed by ultra-sonication in deionized (DI) water, acetone, and isopropyl alcohol. After drying, an ALD SnO_x or nanoparticle SnO_x (*np*-SnO_x) was first deposited onto the precleaned ITO substrate. ALD SnO_x was grown at 190°C in a commercial ALD system (CN-1, Atomic Premium). The precursors used were tetrakis(dimethylamino)tin (TDMASn) and deionized H_2O for the tin and oxygen sources, respectively. The conventional thermal ALD cycle consisted of a dose of TDMASn for 0.5 s, followed by Ar purge of 10 s, followed by a dose of H_2O for 0.1 s, and then Ar purge of 10 s. The plasma-modified ALD cycle as shown in **Figure 1a** was grown at 190°C. The technique consisted of a dose of TDMASn for 0.5 s, followed by Ar purge of 10 s, followed by a dose of Ar plasma for 3 s which is intended to remove ligands and activate the TDMASn surface, followed by Ar purge of 10 s, followed by a dose of TDMASn for 0.5 s, followed by Ar purge of 10 s, followed by a dose of H_2O for 0.1 s, and then Ar purge of 10 s. ALD SnO_x films were

grown for 79 cycles which is approximately 10 nm, and were post-annealed at 150°C for 1 h in air.

Nanoparticle SnO_2 (*np*-SnO_2) solution (diluted with H_2O to 2.5 wt%) were obtained from Alfa Aesar was coated by spin coating at 3000 rpm for 30 s, and the substrates were annealed on a hotplate at 150°C for 1 h. The perovskite solution was prepared by dissolving 800 mg of $FAPbI_3$, 30 mg of MACl, and 30 mg of $MAPbBr_3$ in an DMF/DMSO (8:1 v/v) mixed solvent. The $(FAPbI_3)_{0.95}(MAPbBr_3)_{0.05}$ perovskite solutions were spin-coated onto the ITO/SnO_x substrates at 500 rpm for 5 s, 1000 rpm for 8 s, and 5000 rpm for 12 s, and the ethylacetate in the final spin-stage was dripped onto the substrate during spin coating. After that, the substrates were dried on a hotplate at 100°C for 1 h, 150°C for 4 min. PTAA solutions were prepared in toluene (10 mg/1 mL) with octylammonium bis(trifluoromethylsulfonyl)imide of 2.5 mg. PTAA solutions were spin-coated onto the ITO/SnO_x/$(FAPbI_3)_{0.95}(MAPbBr_3)_{0.05}$ substrates at 3000 rpm for 30 s. Finally, a metal electrode consisting of Au (80 nm) with an area of 9.94 mm^2 was deposited by thermal evaporation in a vacuum for all devices.

1.3 Fabrication of perovskite modules (9-stripe cells connected in series)

The perovskite solar module composed of nine stripes in series on 7 × 7 cm^2 glass/ITO substrates patterned by a laser patterning system (EO TECHNICS). P1 lines were patterned by scribing to separate the ITO substrate with a power of 1.4 W. As transparent electrodes, glass/ITO (indium tin oxide on glass) substrates were prepared by cleaning with a special detergent followed by ultra-sonication in deionized (DI) water, acetone, and isopropyl alcohol. After drying, an ALD SnO_x or nanoparticle SnO_2 (*np*-SnO_2) was first deposited onto the precleaned ITO substrate. ALD SnO_x was grown at 190°C in a commercial ALD system (CN-1, Atomic Premium). The precursors used were tetrakis(dimethylamino)tin (TDMASn) and deionized H_2O for the tin and oxygen sources, respectively. The conventional thermal ALD

cycle consisted of a dose of TDMASn for 0.5 s, followed by Ar purge of 10 s, followed by a dose of H_2O for 0.1 s, and then Ar purge of 10 s. The plasma-modified ALD cycle consisted of a dose of TDMASn for 0.5 s, followed by Ar purge of 10 s, followed by a dose of Ar plasma for 3 s, followed by Ar purge of 10 s, followed by a dose of TDMASn for 0.5 s, followed by Ar purge of 10 s, followed by a dose of H_2O for 0.1 s, and then Ar purge of 10 s. ALD SnO_x films were grown for 79 cycles which is approximately 10 nm, and were post-annealed at 150°C for 1 h in air.

For the modules, nanoparticle SnO_x was coated by shearing (PCM-200, MITSUBISHI ELECTRIC) at 0.5 mm/s followed by thermal annealing at 100°C for 30 min. The perovskite solution was prepared by dissolving 800 mg of $FAPbI_3$, 30 mg of MACl, and 30 mg of $MAPbBr_3$ in an DMF/DMSO (8:1 v/v) mixed solvent. And then the perovskite solution were diluted using same solvent, with volume ratio with 1:0.2 (perovskite solution : solvent). The diluted $(FAPbI_3)_{0.95}(MAPbBr_3)_{0.05}$ perovskite solutions were spin-coated onto the ITO/SnO_x substrates at 500 rpm for 5 s, 1000 rpm for 8 s, and 3000 rpm for 10 s, and the ethylacetate in the final spin-stage was dripped onto the substrate during spin coating. After that, the substrates were dried on a hotplate at 100°C for 1 h, 150°C for 4 min. PTAA solutions were prepared in toluene (10 mg/1 mL) with octylammonium bis(trifluoromethylsulfonyl)imide of 2.5 mg. PTAA solutions were spin-coated onto the ITO/SnO_x/$(FAPbI_3)_{0.95}(MAPbBr_3)_{0.05}$ substrates at 3000 rpm for 30 s. ALD SnO_x/*np*-SnO_x/perovskite/PTAA layers were coated and P2 lines were scribed to expose the bottom ITO substrate to connect the series linkages between cells with a power of 1 W. Finally, Au electrodes formed by thermal evaporation and each sub-modules were separated by laser scribing to form P3 lines with a power of 0.12 W.

1.4 Photocurrent density vs. voltage (*J*-*V*) measurements. Illuminated *J*-*V* characteristics were measured using a Keithley 2420 sourcemeter. The standard 100 mW/cm^2 (1 SUN) illumination was generated by a Newport Oriel Class A 91195A solar simulator using a 450 W

Xe-lamp (Oriel) with an AM 1.5 G filter, while the light intensity was calibrated by a Si-reference cell certified by NREL. The *J-V* curves were measured from 1.5 V to -0.2 V along the reverse scan direction, with a step voltage and scan speed fixed at 10 mV and 150 mV/s, respectively. All devices were measured with a metal mask with an active area of 0.094 cm^2.

1.5 Damp heat test (85ºC and 85% relative humidity). A climatic test was conducted in a chamber (C 4-340 E series, Votschtechnik), and was carried out in a chamber set to a constant temperature (85°C) and constant humidity (85%). The efficiency of the PSCs was measured under illumination at AM 1.5 G after removing the devices from the chamber and cooling them down to room temperature.

1.6 Energy-filtered photoemission electron microscopy (EF-PEEM) analysis. Energy-filtered photoemission electron microscopy (EF-PEEM) was performed under UHV conditions (base pressure of 2×10^{-11} mbar) in the Bristol Ultraquiet NanoESCA Laboratory. Prior to the analysis, the samples were sputtered with 0.5 kV Ar^+ ions (5×10^{-5} mbar) at 45° for 2 minutes (total sputter flux of approximately 9 µA minutes) in a separate preparation chamber to remove surface contaminants. Following preparation, the samples were transferred into the EF-PEEM chamber equipped with a monochromated He I (21.2 eV) excitation light source. The measurements were carried out with an extraction field of 12 kV, 37.6 µm field of view, and at 50 eV pass energy (corresponding to a nominal instrument resolution of 100 meV). A 150 µm contrast aperture was inserted into the back focal plane to improve lateral resolution.

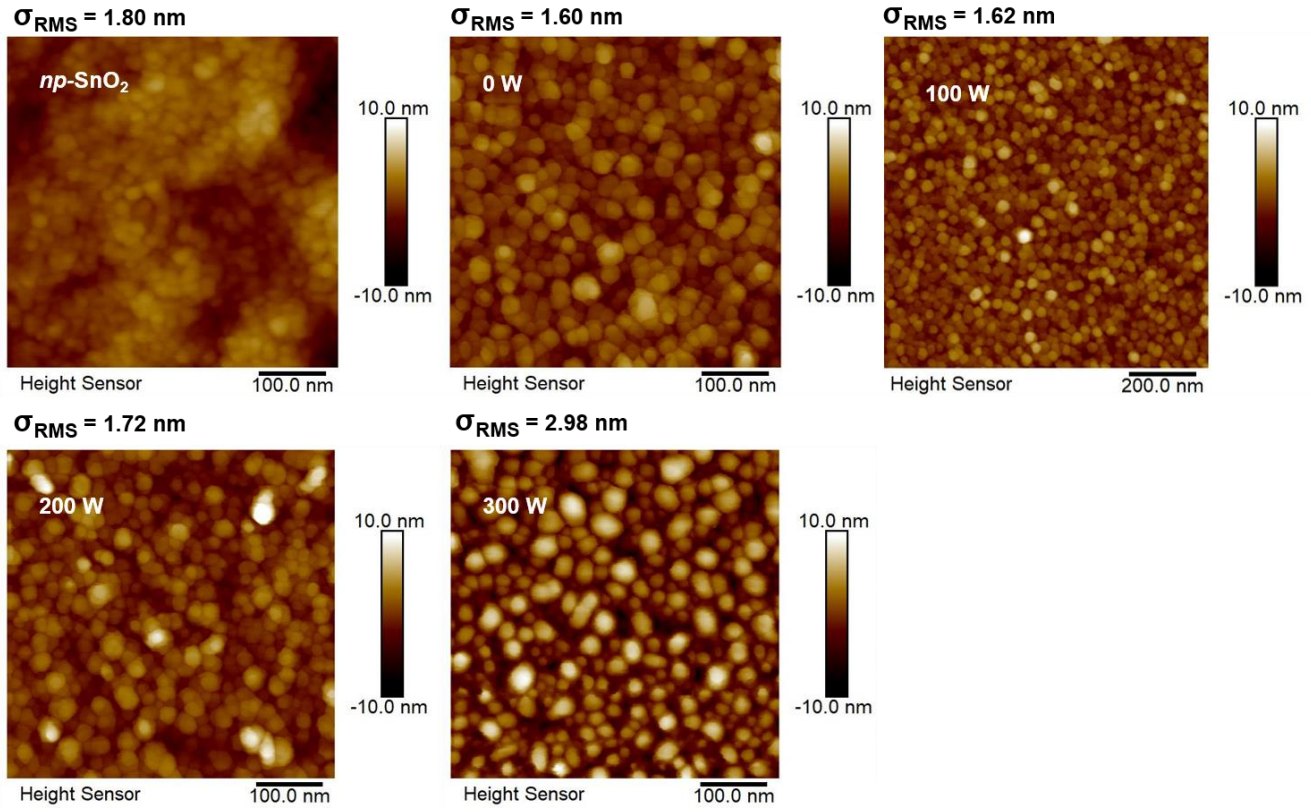

Figure S1. AFM images of the surfaces of the *np*-SnO_2, 0 W, 100 W, 200 W, and 300 W.

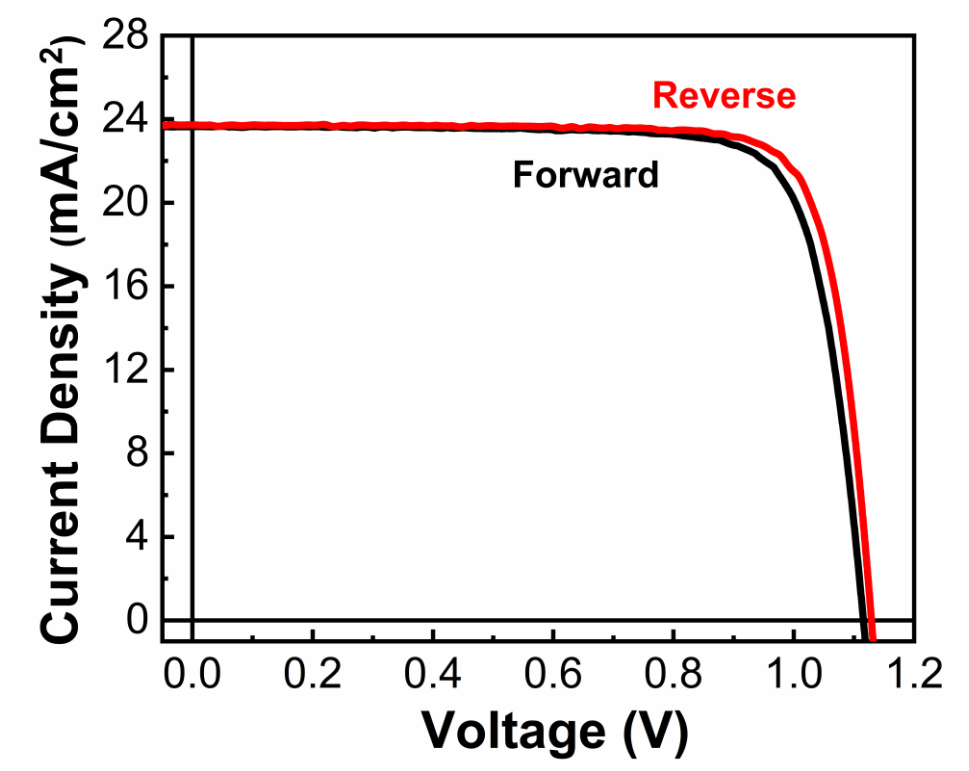

Figure S2. *J-V* characteristics of the photovoltaic device with PMALD SnO_x layer (200 W) under 1 SUN for reverse and forward scans.

Table S1. The photovoltaic device parameters of PMALD SnO_x (200 W) under forward and reverse scans.

	V_{OC} (V)	J_{SC} (mA/cm^2)	*FF* (%)	η (%)
Forward	1.11	23.6	79.4	21.0
Reverse	1.13	23.7	81.5	21.8

Table S2. Photovoltaic parameters. Average perovskite solar-cell performance values for with and without (reference) PMALD SnO_x electron extraction layers deposited with various plasma power.

	J_{SC} (mA/cm^2)	V_{OC} (V)	*FF* (%)	η (%)	R_{SH} (Ω·cm^2)	R_S (Ω·cm^2)
Reference	23.4 ± 0.3	1.07 ± 0.03	77.2 ± 0.9	19.4 ± 0.6	$1.3 \pm 1.8 \times 10^4$	3.6 ± 0.4
0 W	23.6 ± 0.3	1.11 ± 0.00	79.1 ± 0.4	20.7 ± 0.3	$0.5 \pm 0.3 \times 10^4$	3.0 ± 0.1
100 W	23.3 ± 0.1	1.11 ± 0.01	79.1 ± 1.0	20.4 ± 0.4	$1.7 \pm 1.5 \times 10^4$	2.9 ± 0.2
200 W	23.4 ± 0.3	1.13 ± 0.00	80.2 ± 0.9	21.1 ± 0.4	$1.3 \pm 1.5 \times 10^4$	2.8 ± 0.1
300 W	23.2 ± 0.1	0.98 ± 0.08	68.5 ± 3.7	15.6 ± 1.4	$0.5 \pm 0.1 \times 10^4$	6.2 ± 0.7

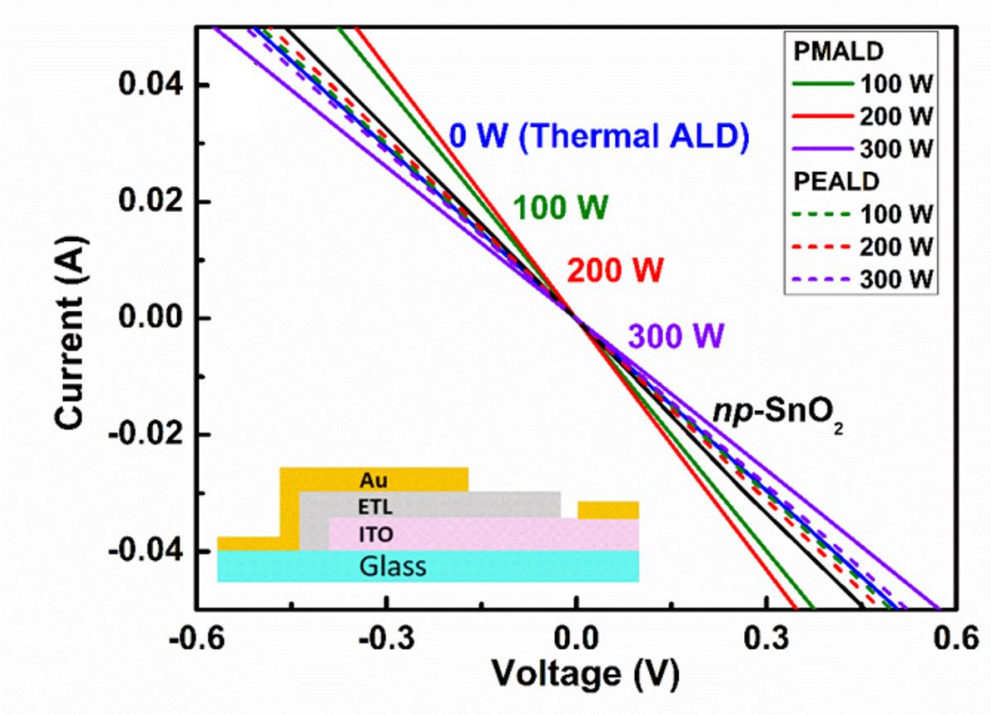

Figure S3. Current vs. voltage (*I-V*) scans of the glass/ITO/SnO_x/Au stacks featuring nanoparticle SnO_2 films (*np*-SnO_2) and SnO_x layers by thermal ALD, PEALD, and PMALD with varying plasma power. These measurements clearly show that the conductance of *np*-SnO_2 spin coated films, thermal ALD and PEALD deposited SnO_x obtained with different oxygen plasma powers are very similar (98.2 ± 5.0 mS). On the other hand, PMALD films show an increase in conductance with increasing plasma power from 137.9 mS (100 W) to 143.6 mS (200 W). Increasing the plasma power to 300 W leads to a decrease in the SnO_x conductance to 86.7 mS.

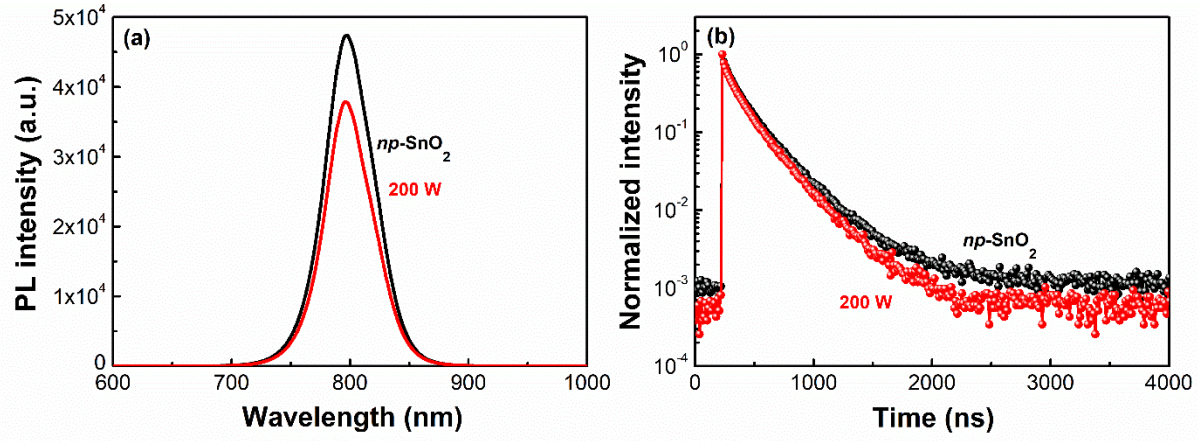

Figure S4. Steady-state photoluminescence (PL) (**a**) and time-resolved PL spectroscopy (**b**) of glass/ITO/ETL/perovskite samples with *np*-SnO_2 (Reference) and 200W PMALD SnO_x. The PL intensity of the perovskite decreased for the PMALD SnO_x with 200 W, in comparison to the reference case, strongly suggesting a more efficient electron extraction. The TRPL data was fitted to a double exponential decay with the fast decay (τ_1), associated with interfacial recombination of free carriers, and the slow decay (τ_2), linked to radiative decay. The TRPL decay times τ_1 and τ_2 are 301.3 and 109.2 ns, respectively, for the *np*-SnO_2 reference, whereas the decay times drop to 252.5 and 85.7 ns for the PMALD SnO_x case with 200 W. Such reduction in the TRPL decay times indicate fast electron transfer from the perovskite film into the PMALD SnO_x film, hence greatly suppressed carrier recombination, leading to enhanced V_{OC}.[1] The enhanced electron transfer from the perovskite film to the PMALD SnO_x is possibly caused by reduced trap density in the perovskite[2-7] and the enhanced conductivity in the PMALD SnO_x compared to the *np*-SnO_2 reference.

Table S3. Photovoltaic parameters. The photovoltaic device parameters of PMALD SnO_x (200 W) with thickness optimization.

PMALD SnO_x 200 W	J_{SC} (mA/cm^2)	V_{OC} (V)	*FF* (%)	η (%)
0 nm (*np*-SnO_2)	23.4	1.10	77.2	19.9
5 nm	23.2	1.10	79.7	20.2
10 nm	23.6	1.10	82.2	21.3
15 nm	23.3	1.10	81.1	20.7
20 nm	23.3	1.10	79.1	20.2

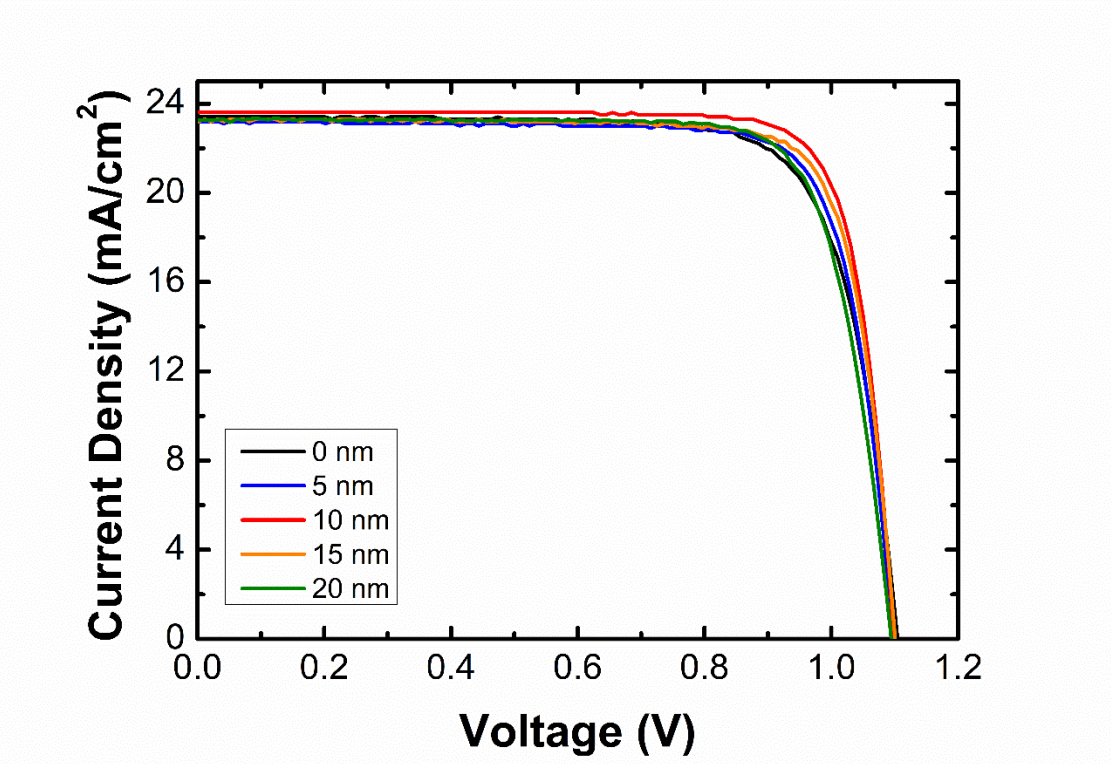

Figure S5. Photovoltaic performance depending on thickness variation. Current density vs. voltage (*J*-*V*) scans of PMALD SnO_x with varying film thickness.

Table S4. Photovoltaic performance parameters of 5 cm × 5 cm modules with a *np*-SnO_2 layer (Reference) and a plasma-modified ALD SnO_x layer (200 W) under 1 SUN.

	J_{SC} (mA/cm^2)	V_{OC} (V)	*FF* (%)	η (%)	R_{SH} (Ω·cm^2)	R_S (Ω·cm^2)
np-SnO_2	2.3	11.1	71.0	17.9	1.3×10^5	5.2×10^2
200W PMALD	2.4	11.4	74.8	20.1	7.1×10^5	4.5×10^2

Table S5. Reports on the efficiency of perovskite solar modules.

ETL	HTL	Active area (cm^2)	V_{OC} (V)	J_{SC} (mA/cm^2)	*FF* (%)	η (%)	Ref.
SnO_2	Spiro	15.03	8.37	3.17	77.97	20.71	Angew. Chem.Int. Ed. **2024**, 63, e2023161.[8]
SnO_2	Spiro	48.00	11.00	-	69.00	18.80	Chemical Engineering Journal **2023**, 456, 140894.[9]
TiO_2	PTAA	45.60	16.07	1.52	75.35	18.45	Nat. Comm. **2022**, 89.[10]
TiO_2	PTAA	30.24	-	-	-	20.99	Joule **2022**, 6, 1689.[11]
TiO_2	Spiro	20.00	12.15	2.29	77.90	21.67	Science **2022**, 375, 302.[12]
TiO_2	Spiro	24.63	10.16	2.75	82.00	22.87	Nat. Nanotech. **2022**, 17, 598.[13]
-	PTAA	27.14	8.715	2.83	75.41	18.60	Nat. Energy **2021**, 6, 633.[14]
-	PTAA	18 (aperture)	5.809	4.25	78.00	19.3	Science **2021**, 373, 902.[15]
TiO_2	PTAA	112	7.64	2.51	72.09	13.82	Joule **2021**, 5, 481-494.[16]
TiO_2	Spiro	23.27	-	-	78.5	20.75	Energy Environ. Sci. **2021**, 14, 4903.[17]
TiO_2	PTAA	42.8	16.05	1.49	70.9	17.05	Nano Energy, **2021**, *82*, p.105685.[18]
TiO_2	Spiro	52	12.03	-	54.9	11.6	Solar Energy Materials and Solar Cells, **2021**, 230, 111189.[19]
TiO_2 /SnO_2	Spiro	21	6.71	3.68	73.44	18.13	Joule **2020**, 4, 1035.[20]
SnO_2	Spiro	13.8	-	-	-	13.1	Solar Energy Materials and Solar Cells, **2018**, 185, 136.[21]
SnO_2	PTAA	16.07	6.54	3.30	69.00	14.89	Nature Communications, **2018**, 9, 4609.[22]
TiO_2	Spiro	36.1	10.2	1.97	75.7	15.7	Nature, **2017**, 550(7674), pp.92-95.[23]
TiO_2	PTAA	40	10.5	2.10	70.16	15.5	J. Mater. Chem. A, **2016**, 4, 17636-17642.[24]
SnO_2	PTAA	23.2	11.3	2.4	74.8	20.1	This work

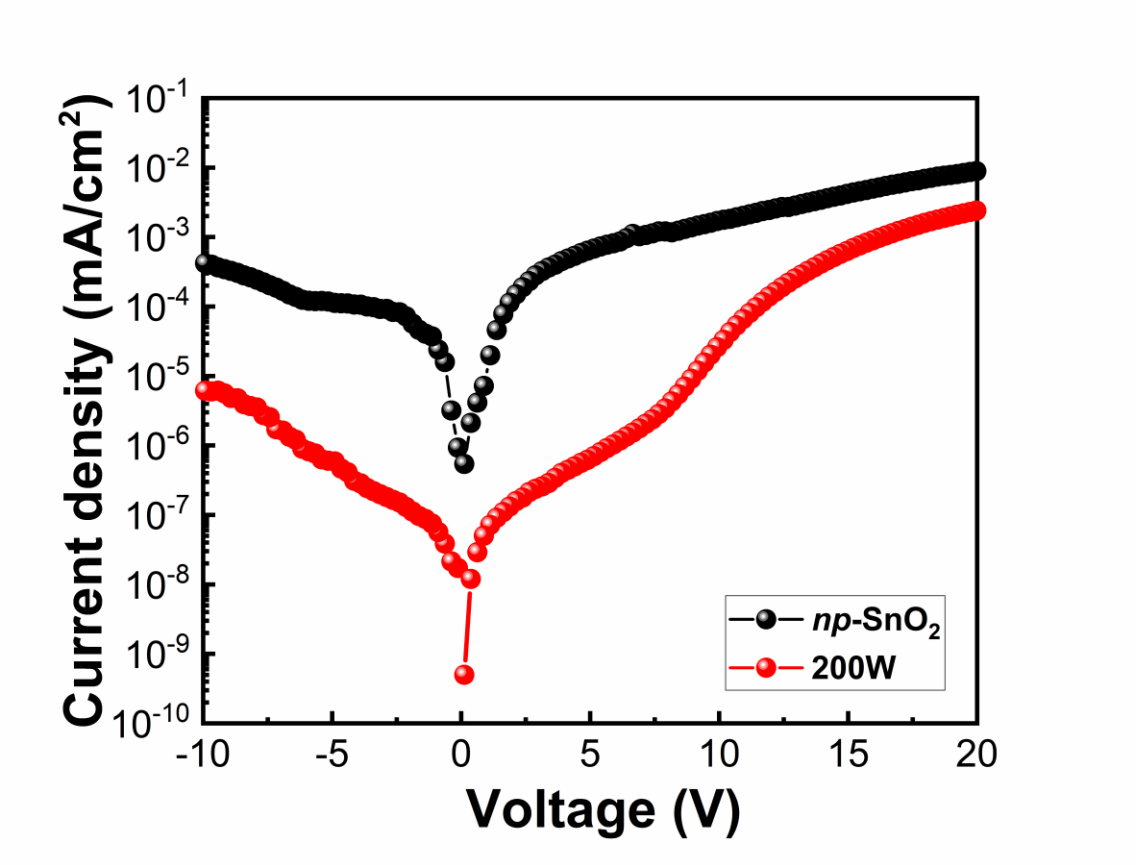

Figure S6. Module dark *J*-*V* curves. 5 cm × 5 cm modules with a *np*-SnO_2 layer (Reference) and upon including a 200 W PMALD SnO_x electron extraction layer.

References

1. Q. Liu, X. Zhang, C. Li, H. Lu, Z. Weng, Y. Pan, W. Chen, X. -C. Hang, Z. Sun, Y. Zhan, *Appl. Phys. Lett*. 2019, **115**, 143903.
2. J. Jiang, Q. Wang, Z. Jin, X. Zhang, J. Lei, H. Bin, Z. -G. Zhang, Y. Li, S. Liu, *Adv. Energy Mater*. 2018, **8**, 1701757.
3. M. Ding, L. Sun, X. Chen, T. Luo, T. Ye, C. Zhao, W. Zhang, H. Chang, *J. Mater. Sci.* 2019, **54**, 12000.
4. T. Niu, J. Lu, R. Munir, J. Li, D. Barrit, X. Ahang, H. Hu, Z. Yang, A. Amassian, K. Zhao, S. Liu, *Adv. Mater.* 2018, **30**, 1706576.
5. X. Meng, J. Lin, X. Liu, X. He, Y. Wang, T. Noda, T. Wu, X. Yang, L. Han, *Adv. Mater.* 2019, **31**, 1903721.
6. S. Song, E. Y. Park, B. S. Ma, D. J. Kim, H. H. Park, Y. Y. Kim, S. S. Shin, N. J. Jeon, T. -S. Kim, J. Seo, *Adv. Energy Mater.* 2021, **11**, 2003382.
7. M. T. Mbumba, D. M. Malouangou, J. M. Tsiba, M. W. Akram, L. Bai, Y. Yang, M. Guli, *J. Mater. Chem. C* 2021, **9**, 14047-14064.
8. H. Yang, T. Xu, W. Chen, Y. Wu, X. Guo, Y. Shen, C. Ding, X. Chen, H. Chen, J. Ding, X. Wu, G. Zeng, Z. Zhang, Y. Li, Y. Li, *Angew. Chem.Int. Ed.* 2024, **63**, e2023161.
9. P. Lv, Y. Yang, N. Li, Y. Zhang, M. Hu, B. Huang, Y. Zhu, Y. Wang, J. Pan, S. Wang, B. Zhang, F. Huang, Y. -B. Cheng, J. Lu, *Chemical Engineering Journal* 2023, **456**, 140894.
10. H. Zhang, K. Darabi, N. Y. Nia, A. Krishna, P. Ahlawat, B. Guo, M. H. S. Almalki, T. –S. Su, D. Ren, V. Bolnykh, L. A. Castriotta, M. Zendehdel, L. Pan, S. S. Alonso, R. Li, S. M. Zakeeruddin, A. Hagfeldt, U. Rothlisberger, A. D. Carlo, A. Amassian, M. Gratzel, *Nat. Comm.* 2022. **89**.

11. J. Xia, Y. Zhang, C. Xiao, K. G. Brooks, M. Chen, J. Luo, H. Yang, N. I. D. Klipfel, J. Zou, Y. Shi, X. Yao, J. Chen, J. M. Luther, H. Lin, A. M. Asiri, C. Jia, M. K. Nazeeruddin, *Joule* 2022, **6**, 1689.

12. M. Kim, J. Jeong, H. Lu, T. K. Lee, F. T. Eickemeyer, Y. Liu, I. W. Choi, S. J. Choi, Y. Jo, H. –B. Kim, S. -I. Mo, Y. -K. Kim, H. Lee, N. G. An, S. Cho, W. R. Tress, S. M. Zakeeruddin, A. Hagfeldt, J. Y. Kim, M. Gratzel, D. S. Kim, *Science* 2022, **375**, 302.

13. Y. Ding, B. Ding, H. Kanda, O. J. Usiobo, T. Gallet, Z. Yang, Y. Liu, H. Huang, J. Sheng, C. Liu, Y. Yang, V. I. E. Queloz, X. Zhang, J. N. Audinot, A. Redinger, W. Dang, E. Mosconic, W. Luo, F. D. Angelis, M. Wang, P. Dorflinger, M. Armer, V. Schmid, R. Wang, K. G. Brooks, J. Wu, V. Dyakonov, G. Yang, S. Dai, P. J. Dyson, M. K. Nazeeruddin, *Nat. Nanotech.* 2022, **17**, 598.

14. Y. Deng, S. Xu, S. Chen, X. Xia, J. Zhao, J. Huang, *Nat. Energy* 2021, **6**, 633.

15. S. Chen, X. Dai, S. Xu, H. Jiao, L. Zhao, J. Huang, *Science* 2021, **373**, 902.

16. J. H. Heo, F. Zhang, C. Xiao, S. J. Heo, J. K. Park, J. J. Berry, K. Zhu, S. H. Im, *Joule* 2021, **5**, 481-494.

17. J. Zhu, S. Park, O. Y. Gong, C. Sohn, Z. Li, Z. Zhang, B. Jo, W. Kim, G. S. Han, D. H. Kim, T. K. Ahn, J. Lee, H. S. Jung, *Energy Environ. Sci*. 2021, **14**, 4903.

18. N. Y. Nia, M. Zendehdel, M. Abdi-Jalebi, L. A. Castriotta, F. U. Kosasih, E. Lamanna, M. M. Abolhasani, Z. Zheng, Z. Andaji-Garmaroudi, K. Asadi, G. Divitini, C. Ducati, R. H. Friend, A. D. Carlo, *Nano Energy* 2021, **82**, p.105685.

19. M. Fievez, P. J. S. Rana, Koh, T. M. Manceau, J. H. Lew, N. F. Jamaludin, B. Ghosh, A. Bruno, S. Cros, S. Berson, S. G. Mhaisalkar, W. L. Leong, *Solar Energy Materials and Solar Cells* 2021, **230**, 111189.

20. J. Li, H. Wang, X. Y. Chin, H. A. Dewi, K. Vergeer, T. W. Goh, J. W. M. Lim, J. H. Lew, K. P. Loh, C. Soci, T. C. Sum, H. J. Bolink, N. Mathews, S. Mhaisalkar, A.

Bruno, *Joule* 2020, **4**, 1035.

21. E. Calabro, F. Matteocci, A. L. Palma, L. Vesce, B. Taheri, L. Carlini, I. Pis, S. Nappini, J. Dagar, C. Battocchio, T. M. Brown, A. D. Carlo, *Solar Energy Materials and Solar Cells* 2018, **185**, 136.
22. T. Bu, J. Li, F. Zheng, W. Chen, X. Wen, Z. Ku, Y. Peng, J. Zhong, Y. -B. Cheng, F. Huang, *Nature Communications* 2018, **9**, 4609.
23. H. Chen, F. Ye, W. Tang, J. He, M. Yin, Y. Wang, F. Xie, E. Bi, X. Yang, M. Gratzel, L. Han, *Nature* 2017, **550(7674)**, pp.92-95.
24. J. H. Heo, M. H. Lee, M. H. Jang, S. H. Im, *J. Mater. Chem. A* 2016, **4**, 17636-17642.